



# Thermodynamic Assessment of Thermochemical Extraction Routes for Titanium Group Metals

Dragan Manasijević\*

University of Belgrade, Technical Faculty in Bor, Serbia

## ARTICLE INFORMATION :

<https://doi.org/10.56801/MMD88>

Received: 17 April 2026

Accepted: 11 June 2026

Type of paper: Research paper



Copyright: © 2026 by the authors, under the terms and conditions of the Creative Commons Attribution (CC BY) license (<https://creativecommons-mons.org/licenses/by/4.0/>).

## ABSTRACT

The thermochemical extraction of titanium group metals (Ti, Zr, Hf) is limited by the extreme thermodynamic stability of their oxides. This study presents a thermodynamic assessment of carbothermic, metallothermic, and halide-based processes using HSC Chemistry 10 software. Ellingham and predominance area diagrams (Ti-C-O, Zr-C-O, Hf-C-O) show that direct carbothermic reduction is inhibited by stable carbide formation, requiring temperatures above 1700 °C for Ti and above 2000 °C for Zr and Hf under high vacuum. Calcium is the only metal considered here that is thermodynamically capable of direct oxide reduction; however, kinetic barriers and product-layer formation limit its practical use. In contrast, carbochlorination lowers the thermodynamic barrier by converting stable oxides into volatile chlorides, which can subsequently be reduced by Mg or Na. This work provides a unified thermodynamic comparison that explains the industrial preference for the Kroll and Hunter processes and identifies favorable operating ranges for titanium group metal extraction.

**Keywords:** titanium group metals; thermodynamic analysis; carbothermic reduction; carbochlorination; phase stability.

## 1. Introduction

Titanium group metals (TGM), comprising titanium, zirconium, and hafnium, are of significant technological importance due to their exceptional combination of mechanical strength, corrosion resistance, and high-temperature stability (Najafzadeh et al. 2024, Djurdjevic et al. 2025). These metals are widely applied in aerospace, automotive, nuclear, biomedical, and chemical industries, where stringent material performance requirements necessitate high purity and controlled microstructure (Boyer 1996, Pushp et al. 2022, Li et al. 2026).

Despite their technological relevance, the extraction of TGM remains challenging (Zhang et al. 2011, Matsanga et al. 2024). The high thermodynamic stability of their oxides ( $\text{TiO}_2$ ,  $\text{ZrO}_2$ ,  $\text{HfO}_2$ ) and their strong affinity for oxygen make direct reduction difficult under conventional conditions. As a result, industrial production relies predominantly on multistep processes, such as chlorination followed by metallothermic reduction (e.g., the Kroll process). Current commercial production is characterized by high energy consumption, environmental pollution, and low efficiency, which has prompted extensive research into alternative thermal reduction and electrolytic methods (Zhang et al. 2011, Takeda et al. 2014, Matsanga et al. 2024). However, the review of current research progress indicates that while several emerging technologies show promise in laboratory and pilot settings, the Kroll

process remains the most widely adopted commercial technology for TGM production (Takeda et al. 2014, Feng et al. 2023).

Thermodynamic analysis provides a fundamental basis for understanding and optimizing extraction processes (Wang et al. 2020). By evaluating the Gibbs free energy changes of relevant reactions and the stability of phases under varying conditions, it is possible to identify feasible reaction pathways and define optimal process parameters. In this context, computational tools enable systematic and consistent evaluation of complex multicomponent systems.

The present study employs HSC Chemistry software (Roine 2026) to perform a thermodynamic assessment of thermochemical extraction routes for titanium group metals. The analysis includes carbothermic, metallothermic, and halide-based processes, with particular emphasis on the influence of temperature and gas-phase composition. By comparing the thermodynamic feasibility and stability domains of key reactions and phases, this work provides a unified basis for evaluating existing technologies and identifying conditions for improved process efficiency and selectivity. Unlike previous reviews that discuss individual extraction routes or focus on a single metal, the present work compares titanium, zirconium, and hafnium extraction under identical calculation conditions. The study systematically compares oxide stability, carbide formation tendencies, chlorination behavior, chloride reducibility, and separation characteristics, thereby establishing a consistent thermodynamic basis for understanding similarities and differences among titanium group metals.

\* Corresponding author.

E-mail address: [dmanasijevic@tfbor.bg.ac.rs](mailto:dmanasijevic@tfbor.bg.ac.rs) (Dragan Manasijević)

## 2. Methodology

Thermodynamic calculations were performed using HSC Chemistry software (version 10.8.0.6) (Roine 2026), which utilizes established thermodynamic databases containing temperature-dependent properties of pure substances and compounds. The analysis focused on the extraction of titanium, zirconium, and hafnium from their respective oxides ( $\text{TiO}_2$ ,  $\text{ZrO}_2$ ,  $\text{HfO}_2$ ). Three principal process routes were investigated:

- carbothermic reduction of oxides
- metallothermic reduction of oxides (using Mg, Na, and Ca as reducing agents)
- halide-based processes involving chlorination of oxides and subsequent reduction

Representative reactions were defined for each route, and their thermodynamic behavior was analyzed over a broad temperature range.

Standard Gibbs free energy changes ( $\Delta G^\circ$ ) of formation reactions for oxides and chlorides as a function of temperature (Ellingham diagrams) were calculated using the H, S, Cp and G Diagrams module of HSC Chemistry. These calculations were used to assess the thermodynamic stability of the studied compounds. Standard Gibbs free energy changes ( $\Delta G^\circ$ ) and standard enthalpy changes ( $\Delta H^\circ$ ) of reduction reactions were calculated using the Reaction Equations module of HSC Chemistry to determine thermodynamic feasibility and heat effects for reduction processes. The results were presented in the form of  $\Delta G^\circ$ -T and  $\Delta H^\circ$ -T diagrams, enabling direct comparison between different reactions.

Predominance area diagrams of Ti-C-O, Zr-C-O, and Hf-C-O systems were constructed using the Stability Diagrams module of HSC Chemistry to evaluate the stability regions of different phases as a function of oxygen and carbon monoxide partial pressures. These diagrams provide insight into the stability domains of oxides, metals, and carbides.

To study the thermodynamics of the oxide carbochlorination process, equilibrium calculations were performed using the Equilibrium Compositions module of HSC Chemistry. The system composition at equilibrium was determined by minimizing the total Gibbs free energy under specified conditions.

All calculations were performed under consistent conditions to enable direct comparison between titanium, zirconium, and hafnium systems. This unified approach allows identification of trends and differences in thermodynamic behavior, particularly with respect to oxide stability, halide formation tendencies, and reducibility. Table 1 presents a summary of representative reactions used in the Gibbs free energy and enthalpy calculations performed in this study. Pure condensed phases were used as standard states, while gaseous species were treated as ideal gases at a standard pressure of 1 bar. The temperature ranges investigated depended on the specific process and are indicated in the corresponding figures and discussions. Equilibrium calculations considered all relevant gaseous and condensed species available in the HSC Chemistry database.

**Table 1.** Summary of representative reactions used in the thermodynamic calculations performed in this study

Reaction type	Representative reaction
Carbothermic reduction	$\text{MeO}_2 + 2\text{C} = \text{Me} + 2\text{CO}(\text{g})$ , Me = Ti, Zr, Hf
Calciothermic reduction	$\text{MeO}_2 + 2\text{Ca} = \text{Me} + 2\text{CaO}$ , Me = Ti, Zr, Hf
Magnesiothermic reduction	$\text{MeO}_2 + 2\text{Mg} = \text{Me} + 2\text{MgO}$ , Me = Ti, Zr, Hf
Sodiothermic reduction	$\text{MeO}_2 + 4\text{Na} = \text{Me} + 2\text{Na}_2\text{O}$ , Me = Ti, Zr, Hf
Chlorination	$\text{MeO}_2 + 2\text{Cl}_2(\text{g}) = \text{MeCl}_4 + \text{O}_2(\text{g})$ , Me = Ti, Zr, Hf
Carbochlorination ( $\text{CO}_2$ )	$\text{MeO}_2 + 2\text{Cl}_2(\text{g}) + \text{C} = \text{MeCl}_4 + \text{CO}_2(\text{g})$ , Me = Ti, Zr, Hf
Carbochlorination (CO)	$\text{MeO}_2 + 2\text{Cl}_2(\text{g}) + 2\text{C} = \text{MeCl}_4 + 2\text{CO}(\text{g})$ , Me = Ti, Zr, Hf
Chloride reduction with Mg	$\text{MeCl}_4 + 2\text{Mg} = \text{Me} + 2\text{MgCl}_2$ , Me = Ti, Zr, Hf
Chloride reduction with Na	$\text{MeCl}_4 + 4\text{Na} = \text{Me} + 4\text{NaCl}$ , Me = Ti, Zr, Hf
Evaporation/Vaporization	Species(condensed) = Species(g), Species = Ti, Zr, Hf, Mg, $\text{MgCl}_2$ , Na, NaCl

## 3. Results and Discussion

### 3.1. Thermodynamic analysis of the feasibility of reduction of titanium group metal oxides

Figure 1 presents the calculated temperature dependence of the standard Gibbs free energy changes for oxide formation reactions of titanium group metals and selected reducing agents (C, Na, Mg, and Ca).

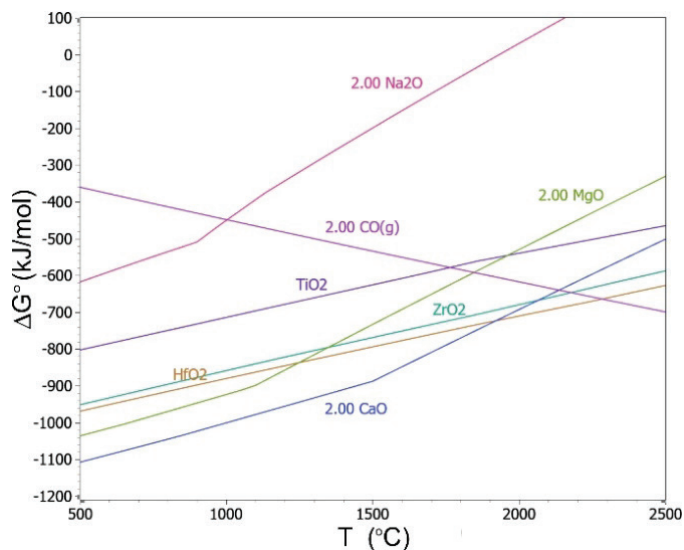


**Fig. 1.** Temperature dependence of standard Gibbs free energy changes for oxide formation reactions of titanium group metals and selected reducing agents (C, Na, Mg, and Ca).

**Table 2.** Standard Gibbs free energy changes ( $\Delta G^\circ$  in kJ/mol) for carbothermic reduction reactions of TGM oxides at different temperatures.

Reaction	$\Delta G^\circ$ (kJ/mol)				
	500 °C	1000 °C	1500 °C	2000 °C	2500 °C
$\text{TiO}_2 + 2\text{C} = \text{Ti} + 2\text{CO}(\text{g})$	442.6	265.7	91.6	-77.8	-234.4
$\text{ZrO}_2 + 2\text{C} = \text{Zr} + 2\text{CO}(\text{g})$	591.6	410.4	234.8	62.1	-111.5
$\text{HfO}_2 + 2\text{C} = \text{Hf} + 2\text{CO}(\text{g})$	609.2	431.9	260.1	92.9	-71.9

The Ellingham-type diagram presented in Figure 1 provides a comparative thermodynamic assessment of oxide stability and reduction potential for titanium group metals (Ti, Zr, Hf) in relation to common reducing agents.

The results clearly demonstrate the exceptionally high thermodynamic stability of  $\text{TiO}_2$ ,  $\text{ZrO}_2$ , and  $\text{HfO}_2$ , as indicated by their strongly negative Gibbs free energy values over the entire temperature range. Among them,  $\text{HfO}_2$  exhibits the greatest stability, followed by  $\text{ZrO}_2$  and  $\text{TiO}_2$ . This trend is consistent with the increasing affinity for oxygen within the group and explains the progressive difficulty in reducing these oxides.

The position of the CO formation line relative to the oxide stability lines indicates that carbothermic reduction is thermodynamically unfavorable under most conditions. Calculated values of standard Gibbs free energy change ( $\Delta G^\circ$  in kJ/mol) for carbothermic reduction reactions of TGM oxides at different temperatures are presented in Table 2. The  $\text{TiO}_2$  line approaches the CO line only at very high temperatures (above approximately 1700 °C), while  $\text{ZrO}_2$  and  $\text{HfO}_2$  do so only at temperatures exceeding 2000 °C, indicating severely limited feasibility. The formation of stable carbides, such as TiC, further complicates metal extraction.

Metallothermic reduction of  $\text{TiO}_2$ ,  $\text{ZrO}_2$ , and  $\text{HfO}_2$  is also very limited (Fig. 1). Sodium forms a relatively unstable oxide ( $\text{Na}_2\text{O}$ ) and therefore does not act as an efficient reducing agent for direct oxide reduction. Its role is instead associated with halide-based processes, where it participates in the reduction of volatile metal chlorides. Magnesium also does not possess sufficient reducing power. Its effectiveness for  $\text{ZrO}_2$  and  $\text{HfO}_2$  reduction is comparatively limited, especially at moderate temperatures. Calcium, forming the most stable oxide ( $\text{CaO}$ ), is the only reductant capable of reducing all three oxides across the entire temperature range considered. However, the industrial implementation of direct calciothermic reduction of  $\text{TiO}_2$  is hindered by the high thermodynamic stability of Ti–O solid solutions, which prevents oxygen removal below the critical solubility limits required for ductility (Suzuki et al. 2003). Additionally, the formation of  $\text{CaO}$  and  $\text{CaTiO}_3$  layers creates a kinetic barrier that prevents complete deoxidation of the titanium core. Furthermore, unlike the magnesium used in the Kroll process, metallic calcium lacks a cost-effective mass-production method suitable for the large-scale reduction of titanium oxides (Takeda et al. 2014).

To further evaluate the feasibility of carbothermic reduction, the predominance area diagrams for the Ti–C–O system at 2000 °C, the Zr–C–O system at 2200 °C, and the Hf–C–O system at 2500 °C (Figure 2a–c) were calculated and analyzed. All systems reveal a common thermodynamic constraint: the high stability of their respective carbides.

In the case of titanium, the reduction path is complicated by the formation of intermediate sub-oxides ( $\text{Ti}_2\text{O}_3$  and  $\text{TiO}$ ) before the metallic state is reached. As shown in the Ti–C–O diagram calculated at 2000 °C, the stability field of metallic Ti is extremely narrow (Figure 2a; stable only at  $\log p_{\text{O}_2} < -15.5$ ). Specifically, the metallic phase is stabilized at very low carbon monoxide pressures ( $\log p_{\text{CO}} < -16$ ), while carbide (TiC) formation dominates at higher  $\log p_{\text{CO}}$  values, with the TiC stability field extending up to  $\log p_{\text{CO}} = 0$  as the oxygen potential increases. At levels close to atmospheric pressure ( $\log p_{\text{CO}} = 0$ ), the system shifts directly from oxides to TiC, avoiding the metallic phase. These conditions require high vacuum to lower  $p_{\text{CO}}$  and stabilize the metal. Similar thermodynamic behavior is observed in the Zr–C–O and Hf–C–O systems (Figure 2b,c). Although these diagrams were constructed at higher temperatures (2200 °C for Zr and 2500 °C for Hf), the stability fields of the metallic phases remain restricted to very low oxygen and carbon monoxide partial pressures. This indicates that, despite the temperature increase, the conditions required for stabilizing the metallic state are still highly demanding.

Therefore, while direct quantitative comparison between the systems is not appropriate due to the different temperatures, the qualitative

trends clearly demonstrate a common thermodynamic limitation. Carbide formation is favored over a wide range of conditions, and the stability of the metallic phase is confined to a narrow region at low  $p_{\text{O}_2}$  and  $p_{\text{CO}}$ .

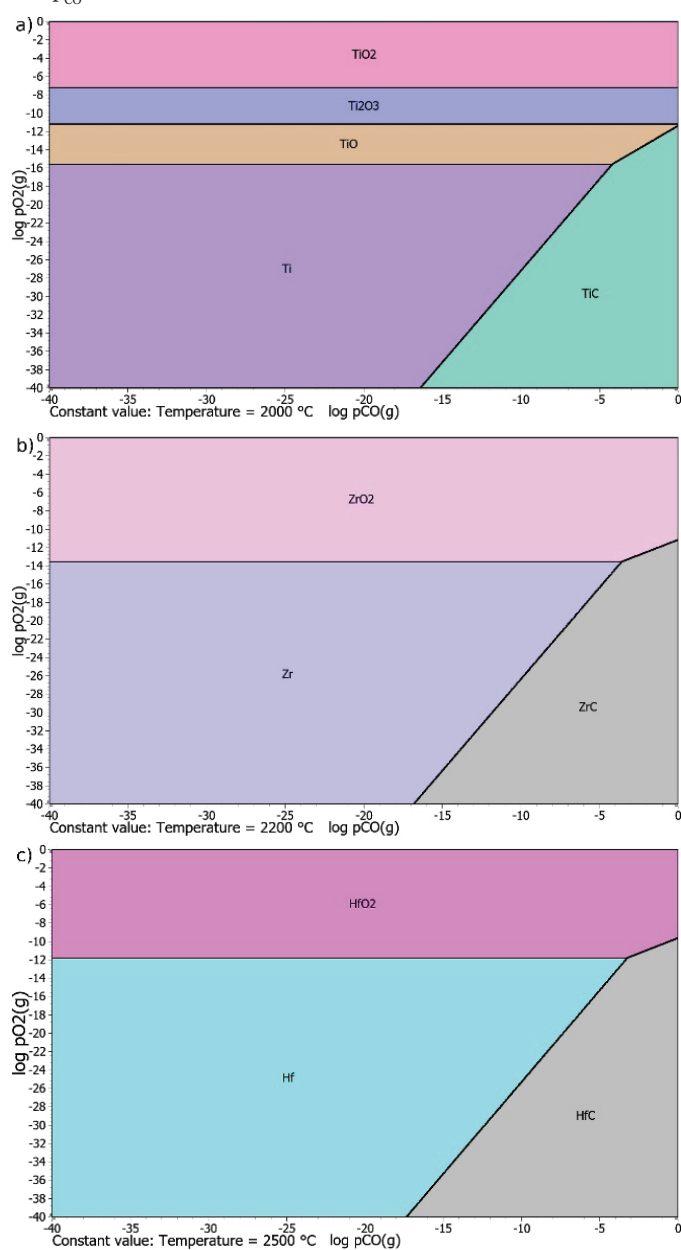


**Fig. 2.** Calculated predominance area diagrams for: (a) Ti–C–O system at 2000 °C; (b) Zr–C–O system at 2200 °C; and (c) Hf–C–O system at 2500 °C. Direct quantitative comparison between Ti, Zr, and Hf is limited because the diagrams were calculated at different temperatures.

Based on this analysis, a unified conclusion can be drawn: carbothermic reduction of  $\text{TiO}_2$ ,  $\text{ZrO}_2$ , and  $\text{HfO}_2$  to pure metals is thermodynamically severely constrained, even at very high temperatures, due to the combined effects of strong oxygen affinity and the high stability of the corresponding carbides.

Overall, this analysis provides a clear thermodynamic justification for the industrial preference for halogenation followed by metallothermic reduction. Chlorination forms volatile intermediates, and subsequent reduction with magnesium or sodium enables extraction while avoiding the limitations imposed by direct oxide reduction. The present analysis is based exclusively on thermodynamic considerations and is therefore intended to identify equilibrium limitations and feasible reaction pathways. Although thermodynamic analysis identifies feasible reaction pathways, thermodynamic favorability alone does not guarantee

industrial applicability. Factors such as reaction kinetics, oxygen diffusion, passivating oxide layers, phase separation, reagent cost, and reactor design can significantly influence process performance. Therefore, the present results should be interpreted as thermodynamic limits rather than direct predictions of industrial behavior.

### 3.2. Thermodynamic analysis of the feasibility of reduction of titanium group metal chlorides

Figure 3 shows the calculated standard Gibbs free energy changes of formation reactions for titanium group metals and Mg, Na, and Ca chlorides as a function of temperature.

The thermodynamic stability of titanium, zirconium, and hafnium chlorides ( $\text{TiCl}_4$ ,  $\text{ZrCl}_4$ , and  $\text{HfCl}_4$ ) is significantly lower than that of their corresponding oxides, as indicated by the less negative values shown in Figure 3. This confirms that chloride-based intermediates are more amenable to reduction. The positions of the  $\text{MgCl}_2$ ,  $\text{NaCl}$ , and  $\text{CaCl}_2$  lines relative to the TGM chlorides indicate that magnesium, sodium, and calcium are thermodynamically effective reducing agents for these chlorides across the investigated temperature range (300–1500 °C). Reduction with sodium forms the basis of the Hunter process, while magnesium reduction underlies the Kroll process, which is widely used for industrial TGM production (Zhang et al. 2011, Takeda et al. 2014, Feng et al. 2023, Matsanga et al. 2024).

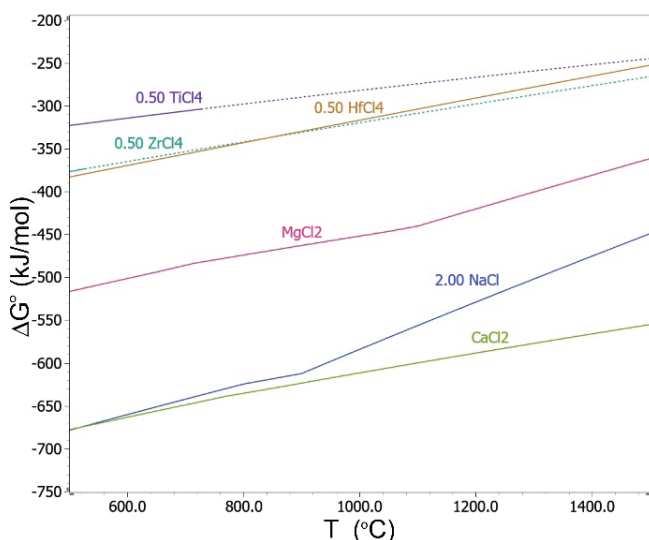


Fig. 3. Standard Gibbs free energy changes of formation reactions for titanium group metals and Mg, Na and Ca chlorides as a function of temperature.

The Kroll process is currently applied more widely than the Hunter process, primarily because titanium separation from  $\text{NaCl}$  is difficult and sodium regeneration is more complex. Since the vapor pressure of  $\text{NaCl}$  is lower than that of  $\text{MgCl}_2$  ( $p_{\text{NaCl}} = 3 \times 10^{-3}$  bar and  $p_{\text{MgCl}_2} = 1 \times 10^{-2}$  bar at 1200 K),  $\text{NaCl}$  separation by distillation is significantly less efficient. Consequently,  $\text{NaCl}$  must be removed by leaching in aqueous solutions, which introduces additional processing steps and increases overall process complexity (Takeda et al. 2014).

In contrast,  $\text{MgCl}_2$  can be more readily separated due to its higher volatility, enabling more efficient recovery and recycling of magnesium. This difference represents a key technological advantage of the Kroll process, contributing to its dominant industrial position despite its own limitations, such as high energy consumption and batch operation (Takeda et al. 2014, Feng et al. 2023).

The Kroll process consists of three main stages: chlorination, reduction, and separation (vacuum distillation). In the chlorination step, titanium-containing feedstock is converted into volatile titanium tetrachloride ( $\text{TiCl}_4$ ), which is subsequently reduced to metallic titanium, followed by separation and purification of the reaction products.

The raw material used for titanium production is typically either

natural rutile, containing about 95%  $\text{TiO}_2$ , or upgraded ilmenite (UGI), in which the  $\text{TiO}_2$  content is increased from an initial value of around 50% through chemical processing. Finely divided rutile or UGI is introduced into a fluidized-bed reactor, where it reacts with chlorine gas in the presence of carbon (coke) at approximately 1000 °C. Under these conditions, titanium is selectively converted into  $\text{TiCl}_4$ , which can be further purified and used as the feed for the subsequent metallothermic reduction stage (Takeda et al. 2014).

### 3.3. Thermodynamic analysis of chlorination process

Titanium was selected as a representative example for the thermodynamic analysis of the chlorination process because the chlorination chemistry of zirconium and hafnium oxides follows analogous thermodynamic trends, while industrial chlorination data are most extensively available for  $\text{TiO}_2$ . Calculated standard Gibbs free energy changes of  $\text{TiO}_2$  chlorination and carbochlorination reactions as a function of temperature are presented in Figure 4.

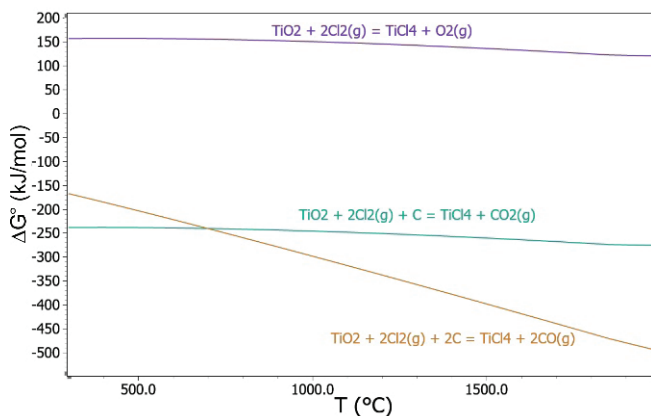
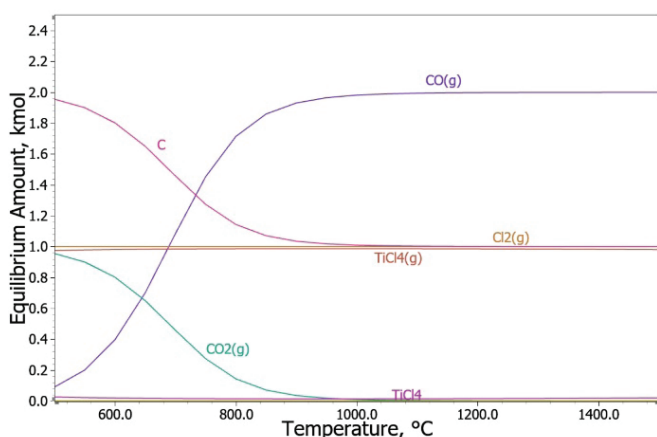


Fig. 4. Standard Gibbs free energy changes of  $\text{TiO}_2$  chlorination and carbochlorination reactions as a function of temperature.

Figure 4 illustrates the critical role of carbon in the chlorination process. Direct chlorination of  $\text{TiO}_2$  (upper line) exhibits positive  $\Delta G^\circ$  values, indicating it is thermodynamically unfavorable under standard conditions. However, the addition of carbon as a reductant (carbochlorination) shifts the equilibrium significantly. The reaction forming  $\text{CO}_2$  is highly spontaneous even at low temperatures, while the reaction forming  $\text{CO}$  becomes increasingly dominant and thermodynamically preferred above approximately 800 °C. This transition justifies the industrial practice of operating carbochlorination reactors at high temperatures to promote rapid kinetics and high conversion to volatile  $\text{TiCl}_4$ .

The equilibrium composition of the 1 kmol  $\text{TiO}_2 + 3$  kmol  $\text{C} + 3$  kmol  $\text{Cl}_2(\text{g})$  system as a function of temperature (500–1500 °C) at 1 bar total pressure is illustrated in Figure 5. The thermodynamic simulation, performed using HSC Chemistry, reveals several important features of the carbochlorination mechanism and the phase stability of the involved species.

The results indicate that the carbochlorination of  $\text{TiO}_2$  is highly favorable across the investigated temperature range. The equilibrium amount of  $\text{TiCl}_4(\text{g})$  remains constant at 1 kmol, corresponding to complete conversion of the initial  $\text{TiO}_2$  feed under the selected equilibrium conditions. This confirms that the Gibbs free energy ( $\Delta G^\circ$ ) for the overall chlorination reaction is significantly negative, even at relatively low temperatures (<600 °C). The most prominent feature of the diagram is the transition between carbon oxidation products ( $\text{CO}_2$  and  $\text{CO}$ ). The transition range between 600 and 1000 °C shows a simultaneous decrease in  $\text{CO}_2$  and  $\text{C}$  concentrations, coupled with a sharp increase in  $\text{CO}$  production. From an industrial perspective, operation above 900 °C favors a  $\text{CO}$ -rich off-gas, which is typical for fluidized-bed chlorinators.



**Fig. 5.** Calculated equilibrium composition for the 1 kmol  $\text{TiO}_2$  + 3 kmol C + 3 kmol  $\text{Cl}_2(\text{g})$  system as a function of temperature.

Thermodynamic simulation of the 1 kmol  $\text{TiO}_2$  + 3 kmol C + 3 kmol  $\text{Cl}_2(\text{g})$  system confirms that carbochlorination is a highly favored process. Equilibrium calculations predict complete conversion under the assumed conditions. However, actual industrial conversion depends on particle size, coke reactivity, chlorine distribution, gas-solid contact efficiency, impurities, and mass-transfer limitations. These findings correlate well with the experimental results reported by Niu et al. (2014) for the chlorination of natural rutile ore. Their study identified 30 wt% petroleum coke as the optimal carbon ratio, which resulted in a  $\text{TiO}_2$  conversion rate of approximately 95% at 950 °C. Furthermore, the residual chlorine predicted in the present calculation supports the common industrial practice of maintaining a stoichiometric excess of chlorine to promote rapid kinetics and high conversion in the presence of impurities.

### 3.4. Thermodynamic analysis of chloride reduction

The thermodynamic feasibility of titanium group metal extraction by halide-based routes was further evaluated through the reduction of their corresponding chlorides. Figure 6 presents the calculated temperature dependence of the Gibbs free energy changes for the reduction of  $\text{TiCl}_4$ ,  $\text{ZrCl}_4$ , and  $\text{HfCl}_4$  with magnesium and sodium.

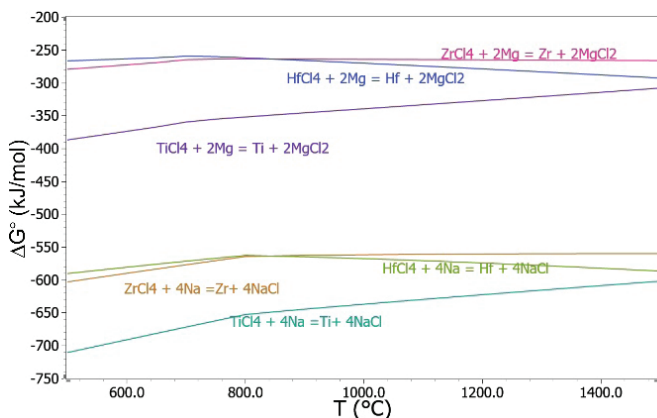


**Fig. 6.** Calculated temperature dependence of standard Gibbs free energy changes for the reduction of  $\text{TiCl}_4$ ,  $\text{ZrCl}_4$ , and  $\text{HfCl}_4$  with magnesium and sodium.

The results indicate that all considered reactions are strongly thermodynamically favorable over the entire investigated temperature range (500–1500 °C), as evidenced by the highly negative  $\Delta G^\circ$  values. This confirms that both magnesium and sodium are effective reducing agents for titanium group metal chlorides. A comparison between the two reductants shows that sodium provides a significantly stronger thermodynamic driving force for reduction. The  $\Delta G^\circ$  values for sodium-based reactions are markedly more negative (approximately –550 to

–700 kJ/mol) compared to those involving magnesium (approximately –250 to –400 kJ/mol). This difference reflects the higher stability of  $\text{NaCl}$  relative to  $\text{MgCl}_2$  and explains the greater reducing potential of sodium.

Among the analyzed systems, the reduction of  $\text{TiCl}_4$  exhibits the most negative Gibbs free energy change for both reductants, indicating that titanium tetrachloride is the most readily reducible species. In contrast,  $\text{ZrCl}_4$  and  $\text{HfCl}_4$  show slightly less negative  $\Delta G^\circ$  values, suggesting marginally lower reducibility, although still highly favorable from a thermodynamic standpoint.

The temperature dependence of  $\Delta G^\circ$  is relatively weak for all reactions, indicating that thermodynamic driving force for reduction remains substantial across a broad temperature interval. This behavior is particularly advantageous for industrial processes, as it allows flexibility in operating conditions without compromising thermodynamic feasibility.

Despite the stronger thermodynamic driving force of sodium, magnesium is preferred in industrial practice (Kroll process), while sodium is used in the Hunter process. This apparent discrepancy arises from differences in physical properties and process considerations rather than thermodynamics alone. As previously discussed, the separation of  $\text{NaCl}$  from titanium is significantly more difficult due to its lower vapor pressure, whereas  $\text{MgCl}_2$  can be efficiently removed by vacuum distillation.

The results confirm that the reduction of titanium group metal chlorides is thermodynamically highly favorable and represents a critical step in modern extraction technologies.

The calculated enthalpy changes for the studied reduction reactions are presented in Figure 7.

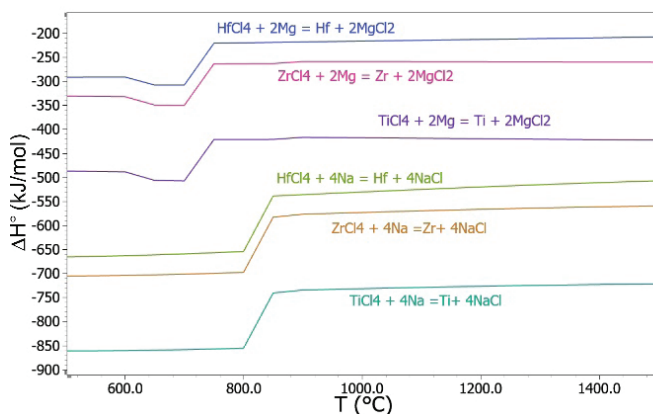


**Fig. 7.** Calculated temperature dependence of standard enthalpy changes for the reduction of  $\text{TiCl}_4$ ,  $\text{ZrCl}_4$ , and  $\text{HfCl}_4$  with magnesium and sodium.

The results show that all investigated reactions are strongly exothermic across the entire temperature range, with  $\Delta H^\circ$  values remaining highly negative, indicating substantial heat release during reduction.

A clear distinction can be observed between sodium- and magnesium-based reductions. Reactions involving sodium exhibit significantly more negative enthalpy values (approximately –550 to –850 kJ/mol) compared to those with magnesium (approximately –250 to –450 kJ/mol). This reflects the higher heat of formation of  $\text{NaCl}$  relative to  $\text{MgCl}_2$  and indicates that sodium reduction is not only more favorable in terms of Gibbs free energy but also considerably more exothermic.

Among the analyzed systems, the reduction of  $\text{TiCl}_4$  shows the most pronounced exothermic effect, particularly in the case of sodium, where  $\Delta H^\circ$  reaches values close to –850 kJ/mol at lower temperatures. Zirconium and hafnium systems follow similar trends, with slightly less negative enthalpy values, consistent with their marginally lower thermodynamic driving forces observed in the Gibbs energy analysis.

### 3.5. Vacuum distillation of titanium, zirconium, and hafnium

Figure 8 presents the calculated saturated vapor pressures of Ti, Zr, Hf, Mg, MgCl<sub>2</sub>, Na, and NaCl as a function of temperature, providing key insight into the separation stage of the Kroll process. The results clearly show that Mg and MgCl<sub>2</sub> exhibit significantly higher vapor pressures than Ti, Zr, and Hf over the entire investigated temperature range. In contrast, all three titanium group metals maintain very low vapor pressures, indicating negligible volatility under the same conditions.

Among the investigated metals, titanium exhibits the highest vapor pressure, followed by zirconium and hafnium. Nevertheless, the vapor pressures of all three metals remain several orders of magnitude lower than those of Mg and MgCl<sub>2</sub>. This pronounced difference in volatility constitutes the thermodynamic basis for vacuum distillation, enabling the selective removal of residual magnesium and magnesium chloride while retaining the metallic product in the condensed phase.

Under reduced pressure (0.1–1 Pa) and elevated temperatures ( $\approx 1000$  °C), Mg and MgCl<sub>2</sub> can be efficiently removed by evaporation, whereas Ti, Zr, and Hf remain essentially non-volatile. These results demonstrate that vacuum distillation is thermodynamically feasible not only for titanium production in the Kroll process but also for the purification of zirconium and hafnium produced via analogous chloride reduction routes.

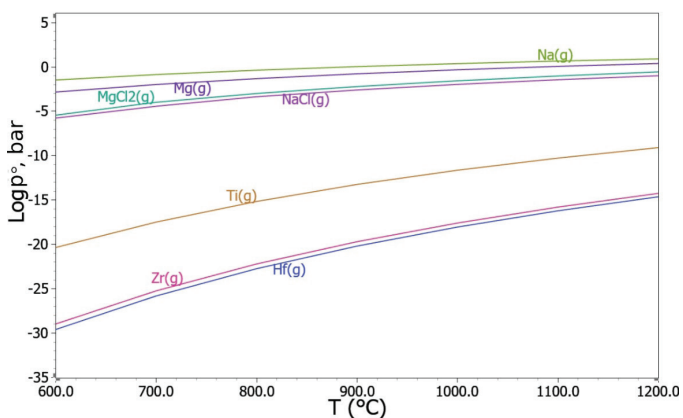


Fig. 8. Calculated saturated vapor pressures of Ti, Zr, Hf, Mg, MgCl<sub>2</sub>, Na and NaCl.

Furthermore, under typical vacuum distillation conditions (approximately 1000 °C), the vapor pressure of MgCl<sub>2</sub>(g) is noticeably higher than that of NaCl(g). This provides the thermodynamic justification for the industrial preference for the Kroll process over the Hunter process, because separation of MgCl<sub>2</sub> by evaporation is substantially more efficient than separation of NaCl, which would instead require aqueous leaching.

The results confirm that the separation step in the Kroll process is thermodynamically well-founded and relies on the favorable volatility differences between the reaction products.

Table 3. Practical summary of favorable process conditions and metallurgical rationale for titanium group metals extraction.

Process stage	Favorable operating condition	Thermodynamic rationale
Carbochlorination	T > 800–900 °C	Shifts the carbon oxidation equilibrium toward CO formation and supports near-complete theoretical conversion of metal oxides to tetrachlorides (MeCl <sub>4</sub> ).
Reductant selection	Mg preferred over Na	Although Na offers a stronger thermodynamic driving force ( $\Delta G^\circ$ ), NaCl has a significantly lower vapor pressure than MgCl <sub>2</sub> , making subsequent vacuum separation less efficient.
Vacuum distillation	T $\approx$ 1000 °C; P = 0.1–1 Pa	Uses the large volatility difference between Mg/MgCl <sub>2</sub> and the metallic sponge phase. Under these conditions, Mg and MgCl <sub>2</sub> evaporate, while Ti, Zr, or Hf remains essentially non-volatile.

### 3.6. Practical Implications and Process Conditions

To connect the thermodynamic calculations presented in this work with industrial practice, a concise summary of favorable operating conditions and core technological choices is compiled in Table 3.

## 4. Conclusion

The present study confirms that the high thermodynamic stability of TiO<sub>2</sub>, ZrO<sub>2</sub>, and HfO<sub>2</sub> represents the primary limitation for direct reduction processes. Carbothermic reduction is fundamentally constrained by carbide formation, which suppresses the stability of the metallic phase even at extreme temperatures.

Metallothermic reduction of oxides is limited to calcium, while magnesium and sodium are ineffective for direct oxide reduction. However, these metals exhibit strong reducing potential toward titanium group metal chlorides, forming the basis of industrial processes.

Carbochlorination is identified as a key step that enables efficient extraction by converting stable oxides into volatile chlorides. Equilibrium analysis predicts complete conversion of TiO<sub>2</sub> to TiCl<sub>4</sub> under the selected calculation conditions, while suppressing carbide formation.

Finally, vapor pressure analysis demonstrates that the separation step in the Kroll process is thermodynamically favorable due to the significant volatility differences between titanium group metals, magnesium, and magnesium chloride.

This analysis offers a clear thermodynamic justification for current technologies and serves as a baseline for future process optimization.

## Acknowledgments

The research presented in this paper was financially supported by the Ministry of Science, Technological Development and Innovation of the Republic of Serbia, within the funding of scientific research work at the University of Belgrade, Technical Faculty in Bor, under contract number 451-03-34/2026-03/20013.

### Conflict of Interest

The author declares no conflict of interest.

## References

- Boyer, R. R. "An Overview on the Use of Titanium in the Aerospace Industry." *Materials Science and Engineering A* 213, no. 1-2 (1996): 103-114. [https://doi.org/10.1016/0921-5093\(96\)10233-1](https://doi.org/10.1016/0921-5093(96)10233-1)
- Djurdjevic, M., S. Stopic, and S. Manasijevic. "Titanium: Abundance, Properties, Recovery from Red Mud and Applications of a Strategic Engineering Material." *Metallurgical and Materials Data* 3, no. 4 (2025): 99-106. <https://doi.org/10.30544/MMD74>
- Feng, Q., M. Lv, L. Mao, B. Duan, Y. Yang, G. Chen, X. Lu, and C. Li. "Research Progress of Titanium Sponge Production: A Review." *Metals* 13, no. 2 (2023): 408. <https://doi.org/10.3390/met13020408>

Li, W., W. Li, J. Hu, P. Liu, H. Shi, and J. Yu. "Investigating the Corrosion Transition Mechanisms of Zirconium Alloys and the Potential Applications of Machine Learning in Predictive Modeling." *Journal of Nuclear Materials* 619 (2026): 156217. <https://doi.org/10.1016/j.jnucmat.2025.156217>

Matsanga, N., M. Wa Kalenga, and W. Nheta. "An Overview of Thermochemical Reduction Processes for Titanium Production." *Minerals* 15, no. 1 (2024): 17. <https://doi.org/10.3390/min15010017>

Najafizadeh, M., S. Yazdi, M. Bozorg, M. Ghasempour-Mouziraji, M. Hosseinzadeh, M. Zarrabian, and P. Cavaliere. "Classification and Applications of Titanium and Its Alloys: A Review." *Journal of Alloys and Compounds Communications* 3 (2024): 100019. <https://doi.org/10.1016/j.jacomc.2024.100019>

Niu, L. P., P. Y. Ni, T. A. Zhang, G. Z. Lv, A. P. Zhou, X. B. Liang, and D. L. Meng. "Mechanism of Fluidized Chlorination Reaction of Kenya Natural Rutile Ore." *Rare Metals* 33, no. 4 (2014): 485-492. <https://doi.org/10.1007/s12598-014-0281-8>

Pushp, P., S. M. Dasharath, and C. Arati. "Classification and Applications of Titanium and Its Alloys." *Materials Today: Proceedings* 54 (2022): 537-542. <https://doi.org/10.1016/j.matpr.2022.01.008>

Roine, A. HSC Chemistry (Version 10.8.0.6). Pori, Finland: Metso, 2026.

Suzuki, R. O., K. Ono, and K. Teranuma. "Calciothermic Reduction of Titanium Oxide and In-Situ Electrolysis in Molten CaCl<sub>2</sub>." *Metallurgical and Materials Transactions B* 34, no. 3 (2003): 287-295. <https://doi.org/10.1007/s11663-003-0038-9>

Takeda, O., T. Uda, and T. H. Okabe. "Rare Earth, Titanium Group Metals, and Reactive Metals Production." In *Treatise on Process Metallurgy: Industrial Processes*, edited by S. Seetharaman, 995-1069. Amsterdam: Elsevier, 2014. <https://doi.org/10.1016/B978-0-323-85373-6.00010-7>

Wang, Z., J. Zhang, B. Zhao, and Z. Liu. "Extraction of Titanium Resources from the Titanium-Containing Waste Slag: Thermodynamic Analysis and Experimental Verification." *Calphad* 71 (2020): 102211. <https://doi.org/10.1016/j.calphad.2020.102211>

Zhang, W., Z. Zhu, and C. Y. Cheng. "A Literature Review of Titanium Metallurgical Processes." *Hydrometallurgy* 108, no. 3-4 (2011): 177-188. <https://doi.org/10.1016/j.hydromet.2011.03.004>